Available online at www.sciencedirect.com

SciVerse ScienceDirect

Energy Procedia 24 (2012) 123 – 130

Energy Procedia

Invited paper

Modeling and control of Multi-terminal VSC HVDC systems

Jef Beerten, Ronnie Belmans

University of Leuven (KU Leuven), Dept. Electrical Engineering (ESAT), Division ELECTA
Kasteelpark Arenberg 10 (bus 2445)
3001 Heverlee, Belgium

Abstract

This paper discusses the modeling and control of Voltage Source Converter High Voltage Direct Current (VSC HVDC) systems in a multi-terminal configuration (MTDC). Both steady-state interactions, as well as transient stability modeling and control are addressed. Simulation results show that adequately modelling the DC voltage droop characteristics or a distributed voltage control in both the power flow algorithm and in the transient stability models allows to simulate the steady-state results of the dynamic simulation by means of power flow software algorithms.

Keywords: VSC HVDC, Multi-terminal HVDC, converter control, DC voltage droop.

1. Introduction

In recent years, the power industry in Europe is showing ever increasing interests in transmission schemes based on High Voltage Direct Current (HVDC) systems. Especially the Voltage Source Converter (VSC) HVDC technology has good prospects for an extension to so-called multi-terminal configurations. The DC side behaves as a voltage source, making power reversal quite straightforward when compared to the Current Source Converter (CSC) technology. Although current day VSC HVDC schemes are all point-to-point connections, the operation principles can be extended to a multi-terminal HVDC (MTDC) system. In recent years, significant research efforts has been put on the modeling and control of VSC MTDC systems as well as interactions with the AC power systems, addressing steady-state interactions using power flow software [1, 2], as well as dynamic interactions by means of simulations in the time domain [3, 4, 5].

This paper discusses the modeling and control of VSC MTDC systems and provides a link between power flow models and the steady-state operation points of transient stability models. Emphasis is put on the interactions in the DC system. Section 2 discusses the operation principles of VSC HVDC converters, as well as recent trends in converter topologies. Sections 3 and 4 respectively discus the steady-state and transient stability models. Finally, section 5 discusses both the steady-state and dynamic interactions by means of simulation results.

 doi:10.1016/j.egypro.2012.06.093

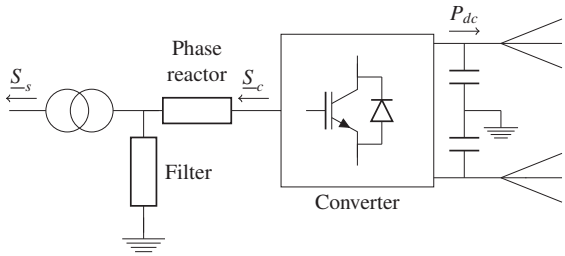

Fig. 1: VSC HVDC converter station.

2. VSC Converter operation and control

In a interconnected AC/DC system, the converters form the connections between the DC systems on the one hand and the AC systems on the other hand. Fig. 1 shows the main components of a converter station connected to a symmetrically grounded monopolar transmission scheme. Contrary to the thyristors used in CSC HVDC technology, the IGBTs in the VSC converters are self-commutated and do not rely on the AC system for commutation. It is therefore possible to connect the VSC converters to existing networks or to start up a remote grid, e.g. in a wind farm, whereas CSC HVDC can only be connected to strong AC networks or need an external voltage source for communication when a connection to a wind farm is considered.

The VSC converters synthesize an AC voltage waveform using a two-level or a multi-level approach. Commercially, these products are available as HVDC Light [6], HVDC PLUS [7] and HVDC MaxSine [8]. The first generations of the HVDC Light technology have been using Pulse Width Modulation (PWM) and a two-level or neutral-point-clamped three-level converter topology, whereas the new converters use a so-called Cascaded Two-Level Converters (CLT) topology [9]. The HVDC PLUS technology uses multilevel switching and is based on the Multi-modular Converter (MMC) approach. The HVDC MaxSine technology uses a hybrid converter concept, with multi-level full H-bridge switching circuits in series with a large number of IGBTs, comparable to the two-level topology. The series cascaded multi-level converter provides a wave shaping function.

Contrary to the two-level topology, all recent developed converter schemes have distributed DC capacitances in the submodules. Dependent on the topology used in the submodules, the converters can either block DC fault currents or rely on an external DC or AC breaker to disconnect in case of a fault on the DC side. Whereas the two-level and three-level topologies can be accurately represented by grouping the cascaded IGBT switches, research on how to accurately model the new multi-level topologies in EMTP-software is ongoing [10].

The earlier two- or three-level schemes use AC filters to remove the high frequency content in the AC voltage waveforms due to the PWM scheme (Fig. 1). In the more recent multilevel schemes, the filter requirements are heavily reduced or even eliminated. When addressing the majority of AC/DC system interactions, in steady-state or dynamically, and under the assumption that the switching behavior is not of particular interest to the problem, the converters can be modeled as a controllable voltage behind a phase reactor.

With respect to the AC or DC grid, each VSC can exhibit a number of different control functions. Due to the decoupled current control, further discussed in section 4, the active and reactive power can be controlled independently since the two orthogonal *dq*-current components can be controlled independently.

With respect to the current component linked with the active power, different control functions can be implemented:

1. P_{ac} *constant*: The converter has a constant active power injection into the AC grid.
2. P_{dc} *constant*: The converter has a constant active power injection into the DC grid.
3. U_{dc} *constant*: The current order is changed to control the DC bus voltage U_{dc} at the converter terminal to a constant value.
4. U_{dc} *droop*: Dependent on the actual value of the DC bus voltage U_{dc}, the current order is changed.

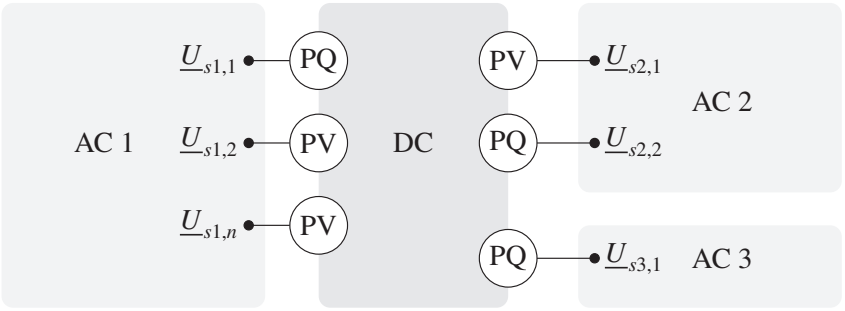

Fig. 2: AC/DC power flow: Representation of converters in the AC power flow.

Dependent on the variable chosen, a linear droop relation can be defined between DC bus voltage and the following quantities:

a) $U_{dc} - I_{dc}$ *droop*: The DC current reference is changed.
b) $U_{dc} - P_{dc}$ *droop*: The DC power reference is changed.
c) $U_{dc} - P_{ac}$ *droop*: The AC power reference is changed.

Using existing control concepts from two-terminal schemes, the $U_{dc} - P_{ac}$ droop option seems the most straight-forward option. From a system's point of view, the $U_{dc} - I_{dc}$ droop relation is the one that is directly linked to the voltage dynamics in the DC system.

With respect to the reactive current component, the following control options can be implemented.

1. *Constant Q*: The converter has a constant reactive power injection Q_s into the AC grid.
2. *Constant U*: The converter adapts the reactive power injection to obtain a constant AC bus voltage magnitude U_s.

When the converter is connected to a remote offshore wind farm, where no external voltage source is available, the converter controls the AC grid voltage magnitude and frequency.

3. Steady-state modeling

Depending on the outer control function implemented in the converter control loop, the steady-state interaction with the AC and DC system has to be modeled differently. This section primarily focuses on the representation of the converters and the resulting model of the DC grid power flow algorithm. More information on the interaction with the AC system and details on the power flow implementation can be found in [2, 11].

With respect to the AC power flow, the VSC stations can be modeled by including them as PV or PQ nodes, as graphically depicted in Fig. 2. When under constant P_{ac} control, the active power P_s injected or withdrawn from the AC grid is known. For the other three control options, an initial estimate is needed to start the iteration process. The initial estimate $P_{s_i}^{(0)}$ can be formulated as:

$$P_{s_i}^{(0)} = \begin{cases} P_{s_i}^{*} & P_{ac} \text{ constant} \\ -P_{dc_i}^{*} & P_{dc} \text{ constant} \\ -\sum_{j=2}^{n} P_{s_j}^{(0)} & U_{dc} \text{ constant} \\ -P_{dc,0_i} \text{ or } P_{s,0_i} & U_{dc} \text{ droop} \end{cases}, \tag{1}$$

with the DC slack bus (U_{dc} constant) the first bus, assuming a DC slack bus to be present. The actual value of P_{0_i} used, depends on whether the droop is implemented as a power-voltage or current-voltage droop, as

defined in the previous section.
After solving the AC grid power flow, the DC powers can be found using

$$P_{dc_i} = -P_{c_i} - P_{loss_i}, \tag{2}$$

with P_{c_i} the converter side power (behind the converter reactor).

The different control strategies implemented can be mathematically represented in the DC grid power flow algorithm by striving to achieve convergence of the controlled quantities to their reference values. The DC grid power flow equations in a monopolar symmetrically grounded scheme can be written as

$$I_{dc_i} = \sum_{\substack{j=1 \\ j\neq i}}^{n} Y_{dc_{ij}} \cdot (U_{dc_i} - U_{dc_j}), \tag{3}$$

$$P_{dc_i} = 2\, U_{dc_i} \sum_{\substack{j=1 \\ j\neq i}}^{n} Y_{dc_{ij}} \cdot (U_{dc_i} - U_{dc_j}). \tag{4}$$

with $Y_{dc_{ij}}$ equal to $1/R_{dc_{ij}}$. In case of a $U_{dc} - I_{dc}$ droop, the current injected by the voltage droop controlled buses, can be written as

$$I_{dc_i} = I_{dc,0_i} - \frac{1}{k_i}(U_{dc_i} - U_{dc,0_i}). \tag{5}$$

Similarly, In case of a $U_{dc} - P_{dc}$ droop, the DC power injected, can be written as

$$P_{dc_i} = P_{dc,0_i} - \frac{1}{k_i}(U_{dc_i} - U_{dc,0_i}). \tag{6}$$

In case of an AC power based droop, the expression becomes similar to (6), but the losses in the converter station have to be taken into account.

In its most general format, in case of both $U - I$ and $U - P$ droop controls implemented on different converters, a vector with unknowns $\boldsymbol{X_{dc}}$ can be defined,

$$\boldsymbol{X_{dc}} = [\underbrace{P_{dc_1}}_{\text{slack}}, \underbrace{P_{dc_2} \ldots P_{dc_k}}_{P-\text{control}}, \underbrace{I_{dc,0_{k+1}} \ldots I_{dc,0_l}}_{U-I\text{ droop}}, \underbrace{P_{dc,0_{l+1}} \ldots P_{dc,0_m}}_{U-P\text{ droop}}, \underbrace{0 \ldots 0}_{\text{outage}}]^T, \tag{7}$$

with the first converter set to DC voltage control (slack), the subsequent $k-1$ converters set to active power control (either constant P_{ac} or P_{dc}) and the remaining operating converters controlling the DC voltage by means of a droop control.

Using this vector of unknowns $\boldsymbol{X_{dc}}$, the DC power flow problem can respectively be rewritten as (8) to be solved with a Newton-Raphson method:

$$\left(\boldsymbol{U_{dc}} \frac{\partial \boldsymbol{X_{dc}}}{\partial \boldsymbol{U_{dc}}}\right)^{(j)} \cdot \frac{\boldsymbol{\Delta U_{dc}}^{(j)}}{\boldsymbol{U_{dc}}} = \boldsymbol{\Delta X_{dc}}^{(j)}. \tag{8}$$

with the mismatch vector $\boldsymbol{\Delta X_{dc}}^{(j)}$ defined as

$$\Delta X_{dc_i}^{(j)} = \begin{cases} P_{dc_i}^{(k)} - P_{dc_i}(\boldsymbol{U_{dc}}^{(j)}) & \forall i\colon\ 2 < i \leq k \\ I_{dc,0_i} - I_{dc,0_i}(\boldsymbol{U_{dc}}^{(j)}) & \forall i\colon\ k \leq i \leq l \\ P_{dc,0_i} - P_{dc,0_i}(\boldsymbol{U_{dc}}^{(j)}) & \forall i\colon\ l \leq i \leq m \\ -P_{dc_i}(\boldsymbol{U_{dc}}^{(j)}) & \forall i\colon\ m < i \leq n \end{cases}. \tag{9}$$

$I_{dc,0_i}(\boldsymbol{U_{dc}}^{(j)})$ and $P_{dc,0_i}(\boldsymbol{U_{dc}}^{(j)})$ can be expressed by rewriting (5) and (6) in terms of respectively $I_{dc,0_i}$ and $P_{dc,0_i}$.

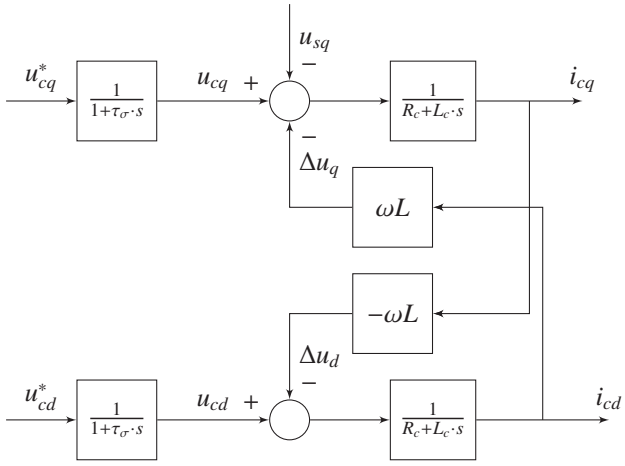

Fig. 3: Transient stability converter model.

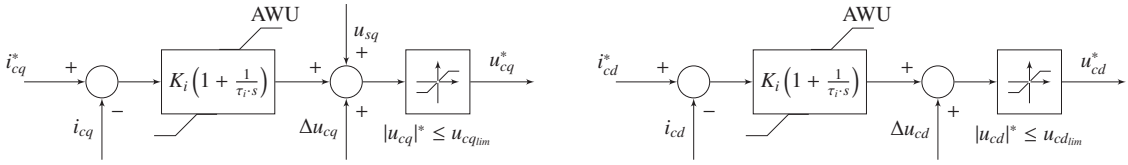

(a) i_{cq} current controller (b) i_{cd} current controller

Fig. 4: Decoupled inner current controllers.

4. Transient stability modeling

Accurately EMTP models of the converters as addressed in section 1 are especially of interest when detailed studies of the DC system dynamics and interactions have to be undertaken. When addressing interactions with large scale AC power system, a transient stability model captures the events of interests in AC power system dynamics while still revealing the necessary details with respect to the DC system interactions. These details of the models form a well balanced trade-off between modeling complexity and computational burden.

From a transient stability point of view, the converter can be modeled in a dq-reference frame as depicted in Fig. 3. The first order system with time constant τ_σ in Fig. 3 represents the time required for the conversion of the reference voltage to the output voltage of the converter due to the converter power electronics [5]. The dynamics of the phase-locked loop (PLL) have been neglected and the grid voltage is oriented according to the q-axis.

Fig. 4 depicts the inner current control loops of the controller. The values of the voltage limits $u_{cd_{lim}}$ and $u_{cq_{lim}}$ and the limits in the anti windup (AWU) scheme depend on the value of the DC voltage u_{dc} on the bus. Priority has to be given to the components in u_c formed by the voltage decoupling terms Δu_{cd} and Δu_{cq} and the contribution due to the grid voltage u_{sq}.

Fig 5 depicts different control structures for the outer q-control loop. As the grid voltage U_s is oriented according to the q-axis, the q-component is related to the active component of the converter current. It is either possible to control the active power injection (Fig. 4(a)), to control the DC voltage to a constant value using a PI-controller (Fig. 4(b)) or to control the DC voltage by means of a voltage droop (Fig. 4(c)), either using a power or current based voltage droop. The current limits $\pm i_{cd_{lim}}$ and $\pm i_{cq_{lim}}$ are related to the maximum current capability of the converter. The d and q-limits are therefore dependent on each other and

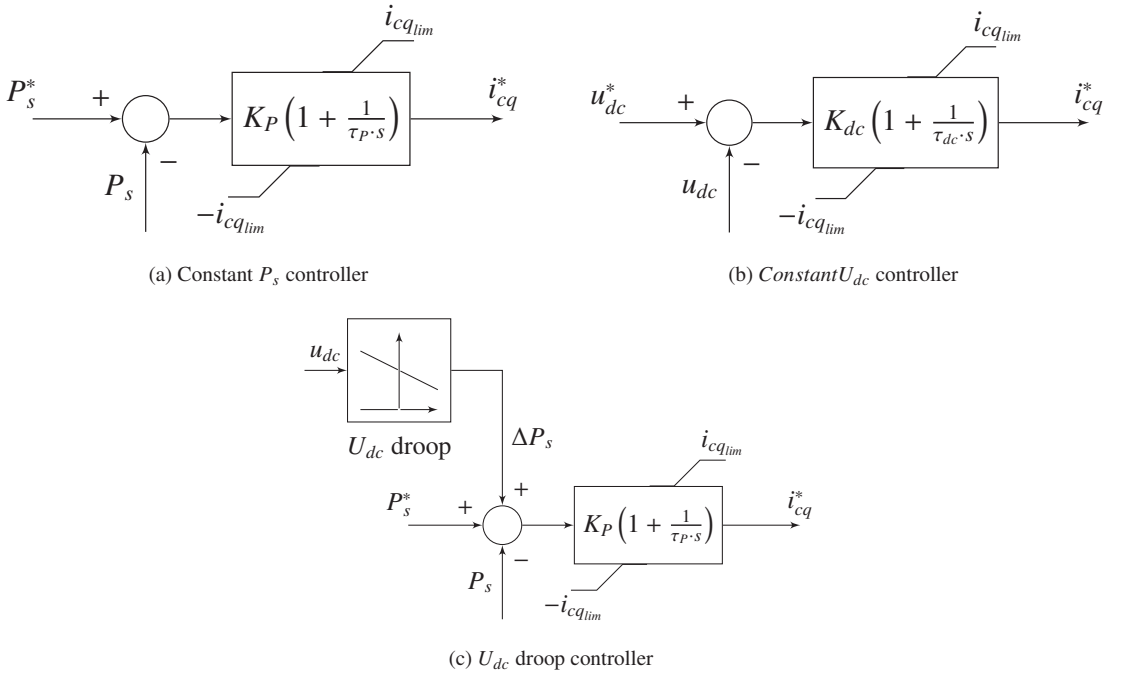

(a) Constant P_s controller

(b) $ConstantU_{dc}$ controller

(c) U_{dc} droop controller

Fig. 5: Outer active power controllers.

priority can be given to active power or reactive power. Alternatively, the converter can keep working with the same power factor when the current is activated.
With respect to the *d*-control loop, the converter can either control the reactive power injected into the AC grid or keep up the AC grid voltage. Similar control structures to Figs. 4(a) - 4(b) can thus be depicted for the reactive power component of the converter current. The steady-state behavior of the converters with respect to the AC and DC system depends on the outer set-points and/or limits hit during the dynamic simulations. When using the steady-state behavior of the DC voltage control in e.g. contingency analysis, the converter limits and droop characteristics have to be implemented in line with the actual implementation in the control loops discussed in this section.

5. Simulation results

When properly modeled, the results from power flow studies are in line with those that result from the dynamic converter control, as discussed in this section. Both steady-state and transient simulations have been carried out on a 4-terminal test system. A MATPOWER implementation using the approach from [2] and the model presented in this paper has been used to obtain the power flow solution. The transient modeling has been performed with MatDyn [12], an open-source toolbox for power system dynamic simulations, using the models described in the previous section. A DC current based droop as addressed in section 3 has been implemented in the power flow package. Converter filters and losses are not included.

All outer *q*-controllers in the transient simulation are based on the droop implementation shown in 5(c), using a current based droop. The converter model and inner current controllers are based on Figs. 3 and 4. The DC lines have been modeled as PI-equivalent cable models, with the inductance of the cable neglected. All AC grids have been modeled as infinite bus systems.

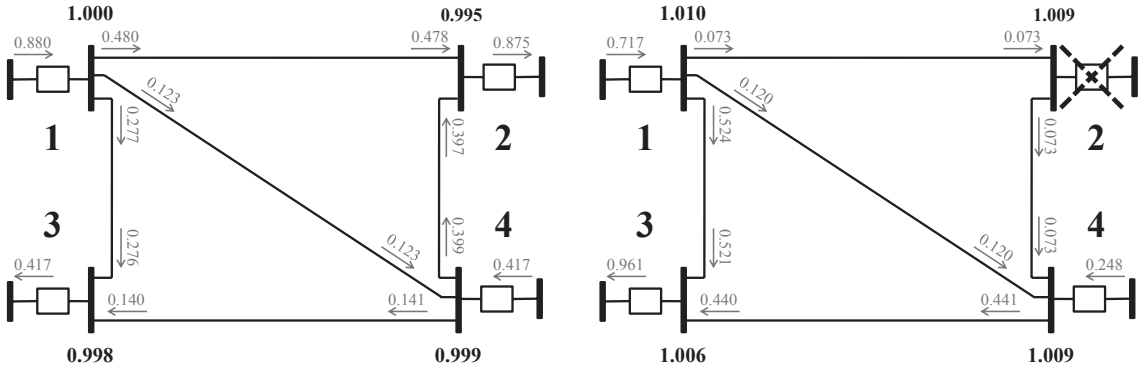

(a) Normal operation (b) Outage of converter 2

Fig. 6: Power flow results before and after outage of converter 2. **Legend**: → Active power (*p.u.*) and voltage **(bold)** (*p.u.*).

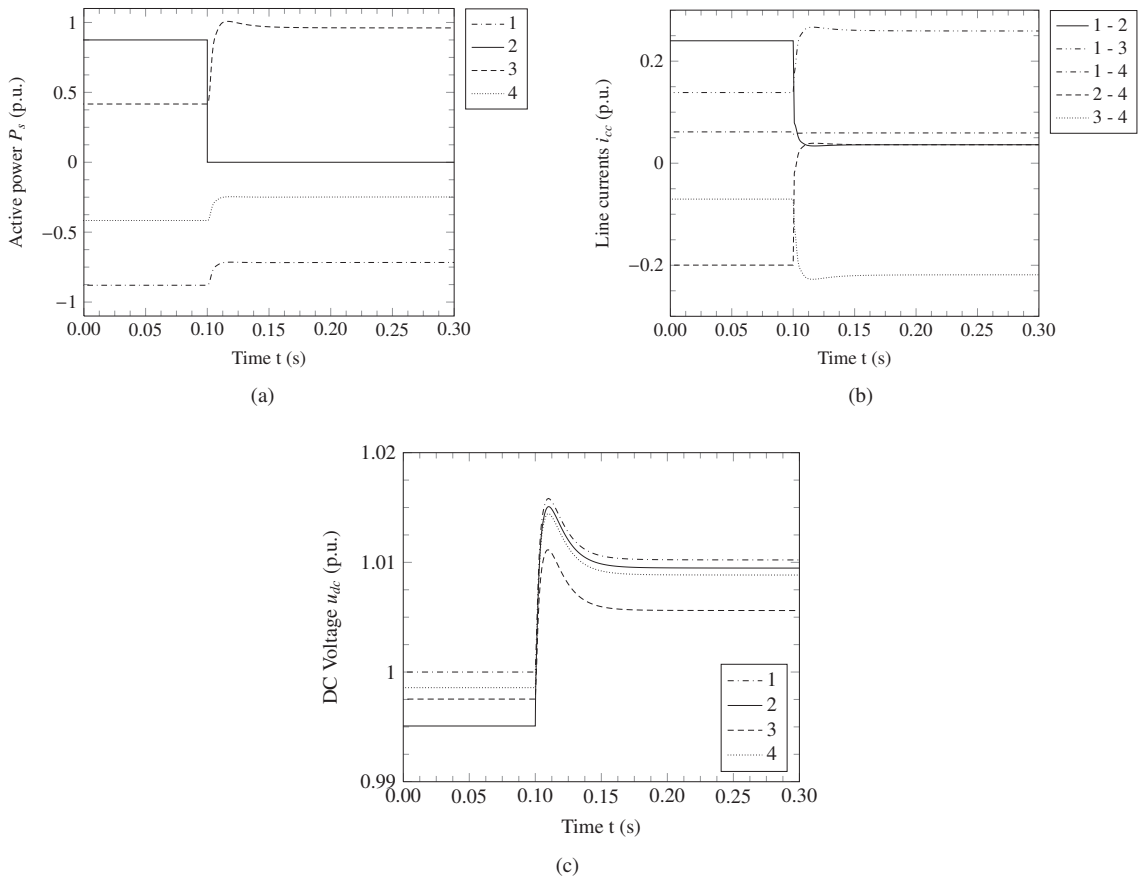

Fig. 7: Dynamic interactions of converters in the DC grid after outage of converter 2: (a) Active power P_s injected into the AC grid, (b) Currents in the DC lines i_{cc} and (c) DC voltage u_{dc} .

Fig. 6 shows the results of the steady-state analysis before and after a outage of converter 2 in the 4-terminal, monopolar symmetrically grounded MTDC system. As expected, the DC voltage and current droop operation points change, as reflected by the results. Fig. 7 shows the results of the dynamic analysis. Due to the selection of power and voltage base, the DC line currents in the symmetrically grounded system are about half of the line powers in Fig. 6. With droop settings and an implementation similar in the power flow and transient model, the results of the power flow analysis are in line with the steady-state results of the dynamic simulations.

It is clear from the results that, when properly modeled, the AC/DC power flow algorithm can be used to analyze the steady-state interactions of the droop-controlled converters. As addressed in [11], this also impacts the power flows in the AC systems.

6. Conclusion

In this paper, the steady-state and dynamic modeling of VSC MTDC systems has been discussed. The implementation of the voltage droop characteristics in steady-state power flow algorithms allows to extend contingency analyses to DC grids and to study the effects of the droop control and the individual droop values of each converter on the post-disturbance power flows in both the AC and DC system. The transient model allows to study the dynamic interactions of the converters and the effect of the individual droop values. Similarly, the transient model can be included in an AC transient stability program, allowing to study the dynamic interaction of the AC and DC system.

Acknowledgement

Jef Beerten is funded by a research grant from the Research Foundation – Flanders (FWO).

References

[1] A. Pizano-Martinez, C. R. Fuerte-Esquivel, H. Ambriz-Perez, E. Acha, Modeling of VSC-based HVDC systems for a Newton-Raphson OPF algorithm, IEEE Transactions on Power Systems 22 (4) (2007) 1794–1803.

[2] J. Beerten, S. Cole, R. Belmans, Generalized steady-state VSC MTDC model for sequential AC/DC power flow algorithms, IEEE Transactions on Power SystemsAccepted for publication.

[3] L. Zhang, L. Harnefors, H.-P. Nee, Modeling and control of VSC-HVDC links connected to island systems, IEEE Transactions on Power Systems 26 (2) (2011) 783–793.

[4] T. M. Haileselassie, K. Uhlen, J. O. Tande, O. Anaya-Lara, Connection scheme for north sea offshore wind integration to UK and Norway: Power balancing and transient stability analysis, in: Proc. IEEE Trondheim PowerTech, 2011, pp. 1–5.

[5] S. Cole, J. Beerten, R. Belmans, Generalized dynamic VSC MTDC model for power system stability studies, IEEE Transactions on Power Systems 25 (3) (2010) 1655–1662.

[6] P. Haugland, It's time to connect - technical description of HVDC Light technology, Tech. rep., ABB (March 2008).

[7] K. Friedrich, Modern HVDC PLUS application of VSC in modular multilevel converter topology, in: Proc. IEEE Int Industrial Electronics (ISIE) Symp, 2010, pp. 3807–3810. doi:10.1109/ISIE.2010.5637505.

[8] N. M. MacLeod, C. D. Barker, A. J. Totterdell, From concept to reality; the development of a multi-level VSC HVDC converter, in: CIGRE 2011 Bologna Symposium, Bologna, Italy, 2011.

[9] B. Jacobson, P. Karlsson, G. Asplund, L. Harnefors, T. Jonsson, VSC-HVDC transmission with cascaded two-level converters, in: Proc. CIGRE 2010, Paris, France, 2010.

[10] U. N. Gnanarathna, A. M. Gole, R. P. Jayasinghe, Efficient modeling of modular multilevel hvdc converters (mmc) on electromagnetic transient simulation programs, IEEE Transactions on Power Delivery 26 (1) (2011) 316–324. doi:10.1109/TPWRD.2010.2060737.

[11] J. Beerten, D. Van Hertem, R. Belmans, VSC MTDC systems with a distributed DC voltage control – a power flow approach, in: Proc. IEEE PowerTech '11, Trondheim, Norway, 2011.

[12] S. Cole, R. Belmans, Matdyn, a new matlab-based toolbox for power system dynamic simulation, IEEE Transactions on Power Systems 26 (3) (2011) 1129–1136.